

## A High Power High Energy Pure N<sub>2</sub> Laser in the First and Second Positive Systems

F. Encinas Sanz and J. M. Guerra Perez

Departamento de Optica, Facultad de Ciencias Físicas, Universidad Complutense, E-28040 Madrid, Spain

Received in revised form 25 April 1990/Accepted 9 August 1990

**Abstract.** Simultaneous high energy lasing in the N<sub>2</sub> first and second positive systems is reported. 20.5 mJ (1.5 MW) UV and 5 mJ (0.4 MW) IR laser pulses were produced in pure N<sub>2</sub>. The design is open and easy to improve.

**PACS:** 42.55.Em, 42.60.By

The most popular excitation schemes in transversely pumped N<sub>2</sub> lasers are the charge transfer and the Blumlein type circuitry. Although both systems have similar potentialities, in recent years the higher power [1], energy [2] and efficiency [3] have been attained with various versions of charge transfer schemes.

The conditions necessary to obtain a good performance seem to be a little more stringent in a Blumlein type excitation system than in the charge transfer one. Both circuits use two capacitors and one spark-gap (Fig. 1). In a Blumlein circuit both capacitors are initially charged at the same potential  $V_0$ . When the spark-gap is fired, one capacitor is discharged and the laser gap is overvolted. If the breakdown is not produced before and the reactive circuit elements are the only ones considered, the maximum voltage between the electrodes in the main gap is  $2V_0$ . Then the second capacitor discharges to the first one through the laser gap. A low rise time in the current across the laser gap is essential in order to get an efficient laser emission.

To fulfill this condition, the spark-gap and both capacitors must have a very low internal inductance and be closely coupled to the laser gap [4]. Thus, both capacitors are usually flat lines (typical inductance  $\cong 0.1$  nH).

In the charge transfer excitation, only one capacitor is coupled directly to the laser gap. Therefore, the conditions of close coupling and low inductance mainly affect this capacitor, whereas the characteristic of the storage capacitor and its coupling through the spark-gap are far less influential. If the breakdown has not occurred before, the maximum voltage is  $2V_0(1 + C_p/C_s)^{-1}$ . If the peaking capacity  $C_p$  is much lower than the storage capacity  $C_s$ , the maximum voltage approaches to  $2V_0$  as in the

Blumlein scheme. These considerations may justify the choice of a charge transfer excitation system for attaining maximum power, energy and efficiency.

Here we study a high power, high energy N<sub>2</sub> laser with charge transfer excitation. Working with pure N<sub>2</sub> in our laser we have measured 5 mJ (400 kW) energy per pulse in the infrared first system and 20.5 mJ (1.5 MW) in the ultraviolet (337 nm) second system. The infrared output is four times the maximum power reported in the literature [5]. The UV output energy is similar to the highest reported [1, 2, 5, 6].

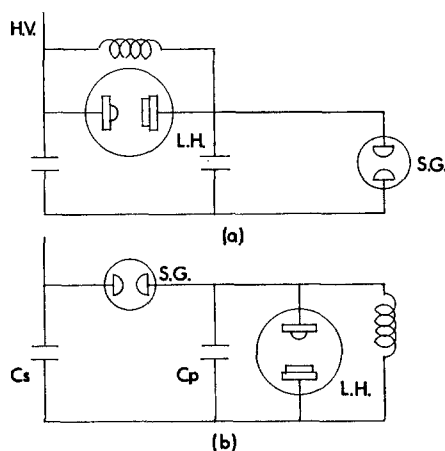


**Fig. 1a, b.** Electric circuits: **a** Blumlein excitation. **b** Charge transfer excitation. L.H. laser head,  $C_s$  storage capacitor,  $C_p$  peaking capacitor, S.G. spark-gap

## 1. Experimental Design

The mechanical construction of the laser is shown in Fig. 2. The gas envelope of the laser is a PVC structure in which the coupling inductance is reduced by screwing it directly on to the metallic plates supporting the electrodes. Both electrodes are easily exchangeable. The upper electrode exhibits a cylindrical profile (1 cm diameter) and the lower one is flat. Both were rounded at the ends, to avoid the generation of sparks channels. Thus, the overall estimated length of the discharge is 65 cm. The spark-gap SG and the storage capacitor  $C_s$  are directly mounted on to the support plate of the upper electrode. The close coupled (peaking) capacitor  $C_p$  consisted in two flat plates made of a fiber glass epoxy laminate faced with copper foil. They are connected to the upper and lower electrodes by a thin copper sheet covering the entire length. In the same way, the upper contact of the storage capacitor is connected to the grounded sheet of both capacitor plates. Symmetry and low coupling inductance were the two main guidelines used in the mechanical construction.

The electrical excitation circuit is practically the same charge transfer system described in [3] (Fig. 1b).

A parallel arrangement of four 50 nF low stray inductance commercial capacitors or one 200 nF capacitor were alternatively used for storage. They were screwed directly onto the two electrodes low inductance spark-gap. The spark-gap is fired by releasing the filler gas pressure. The storage capacitor was charged to a maximum of 32 kV. High grade purity N<sub>2</sub> filled the discharge chamber.

The UV + IR pulseform was measured with a rapid (rise time  $\leq 1$  ns) photodiode and the isolated UV with a short rise time ( $\leq 100$  ps) planar photocell. The pulse energy was measured by a thermopile with calibration traceability to the National Bureau of Standards. Current and voltage transients were monitored by low rise time probes. Optical and electrical probes were coupled by a 50  $\Omega$  line matched to a 500 MHz nominal bandwidth transient programmable digitizer. All the electronic measurement devices and light detectors were placed in a Faraday cage.

The optical resonator consisted of a flat metallic full reflector and an uncoated flat quartz output coupler.

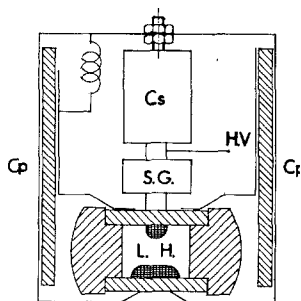


Fig. 2. Mechanical construction of the N<sub>2</sub> laser. L.H. laser head,  $C_s$  storage capacitor,  $C_p$  peaking capacitor, S.G. spark-gap

## 2. Laser Performance

The UV laser pulse and the results of the electrical measurements are summarized in the set of waveforms registered; these are shown in Fig. 3. All the probes were coupled to the transient digitizer with matched cables for which the signal transit times were equalized. Thus, the different waveforms in Fig. 3 are synchronized. For checking the discharge system, the current waveform produced by the close coupled peaking capacitor  $C_p$  is important. The total inductance in the loop containing the peaking capacitor and the laser gap is extracted from this signal. With the 40 nF peaking, the measured inductance is 5 nH, the peak current 80 kA and the peak voltage 30 kV. All the waveform peaks are simultaneous with the UV radiation peak as is shown in Fig. 3. The instantaneous channel resistance in the UV laser emission peak is then estimated to be 0.4  $\Omega$ . The N<sub>2</sub> pressure was 60 Torr when the waveforms in Fig. 3 were registered.

The inductance  $L_s$  of the storage capacitor  $C_s$  was also obtained from the second period in the voltage oscillation [7]. Thus, the stray and coupling inductance for the parallel arrangement of four 50 nF capacitors was  $(L_s)_1 = 140$  nH and for one single 200 nF capacitor  $(L_s)_2 = 190$  nH. In spite of the difference in inductance between the two storage capacitors the laser output is reduced by only 10% with the single 200 nF storage capacitor. This shows that the stray inductance of the storage capacitor is relatively less important.

To obtain a high UV pulse energy it is very important to have the resonator carefully aligned (Fig. 4). But in this case, simultaneous lasing is produced in the UV and IR positive systems (Fig. 5). To isolate the IR output, a UV absorbing filter is placed in front of the thermopile or the photodiode. In the high energy laser described in [2] the resonator was also carefully aligned and it is possible that a sizeable fraction of the energy detected by the used thermopile may also be infrared and not only ultraviolet

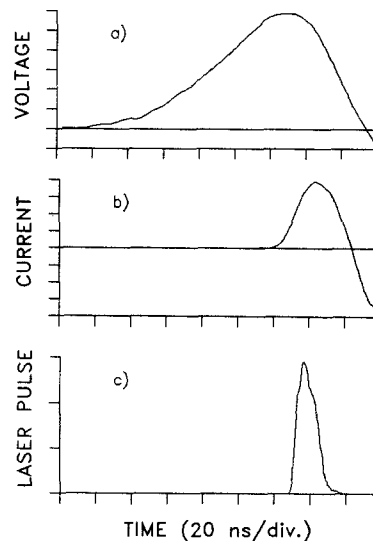


Fig. 3a-c. Pulse correlation. a Electrode voltage (5 kV/div.), b Peaking capacitor discharge current (20 kA/div.), c UV laser pulse. Electrode gap  $d = 4$  cm,  $C_p = 40$  nF

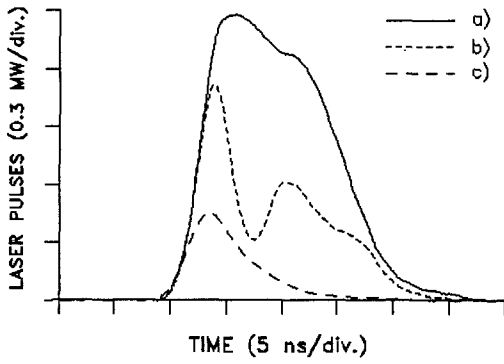


Fig. 4. Resonator and alignment influence in the UV laser pulse. *a* Aligned resonator, *b* Output quartz window with a  $2^\circ$  offset alignment, *c* Suppressed resonator.  $d=4$  cm,  $C_p=40$  nF

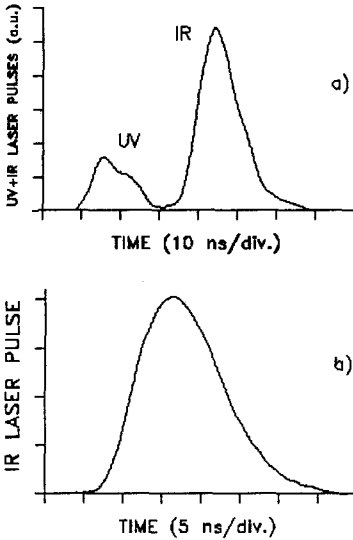


Fig. 5. *a* UV and IR laser pulses.  $d=4$  cm,  $C_p=20$  nF and  $P=60$  Torr. *b* IR laser pulse.  $d=4$  cm,  $C_p=40$  nF and  $P=60$  Torr

output as assumed implicitly by the authors. Perhaps this behaviour has gone by unnoticed in other reports on high energy UV  $N_2$  lasers.

Brass, stainless steel and copper electrodes were tested without any noticeable difference in laser performance. No attempt was made to improve the diameter of the upper electrode which was always 1 cm.

The separation between the electrodes was changed from 1 to 4 cm. The pulse energy shows an almost linear increase with the separation (Fig. 6). The breakdown voltage also grows with the separation starting at 18 kV at 1 cm and reaching 30 kV at 4 cm. The separation was not greater than 4 cm, because of limitations in the construction of the PVC structure. This behaviour is not very surprising because the maximum energy deposition rate (power) on the plasma is produced when the driven circuit impedance  $Z_d$  and the plasma impedance  $Z_p$  are in the ratio  $Z_p/Z_d=2$ . In our case with  $L=5$  nH and  $C_p=40$  nF,  $Z_d \cong (L/C_p)^{1/2} = 0.35 \Omega$  and  $Z_p$  can be taken to be  $Z_p \cong R_p(t)|_{\text{laser peak}}$ . When the interelectrode distance is 4 cm we have  $R_p \cong 0.4 \Omega$  and the matching is produced at a distance in which  $R_p=2Z_d \cong 0.7 \Omega$ . Moreover as the breakdown voltage grows with the interelectrode dis-

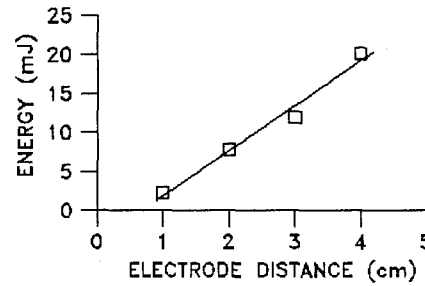


Fig. 6. UV output energy vs electrode distance.  $C_p=40$  nF,  $P=60$  Torr

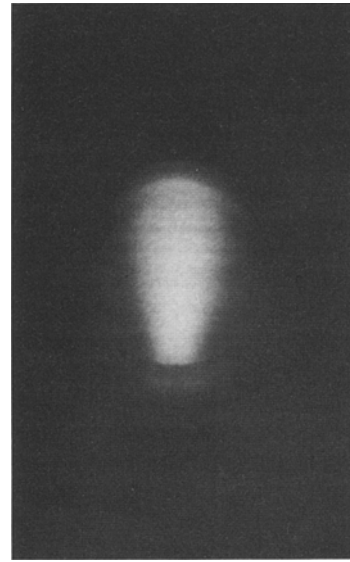


Fig. 7. Photograph of the fluorescence produced by the laser spot

tance, the energy transferred to the peaking capacitor and afterwards to the plasma also grows.

No preionization system such as grooves or mesh electrodes was included in the design. In spite of such simplicity, the pulse-to-pulse reproducibility was better than 10% in one single energy pulse measurement. Also the beam quality is good with a cross section of  $40 \times 10$  mm in the near field (Fig. 7).

Working at a pressure of 50 Torr, the peaking capacity  $C_p$  was varied between 1 and 40 nF. The storage capacitor and the charging voltage were kept constant ( $C_s=200$  nF and  $V_c=30$  kV). The pulse energy grew steadily with the peaking capacity  $C_p$ , both in the UV and IR outputs (Fig. 8) without reaching saturation when  $C_p=40$  nF. Thus, in principle it should be easy to raise the output pulse energy with higher values of  $C_p$ , not used in our set-up due to mechanical limitations which should not be difficult to overcome. In the second positive system the population inversion is obtained via direct electronic impact excitation. Then the output laser intensity is expected to be proportional to the current maximum  $i(t)|_{\text{max}} \cong V_c(C_p/L)^{1/2}$  where  $V_c$  is the peaking capacitor charging voltage.  $V_c$  is also the breakdown voltage, which

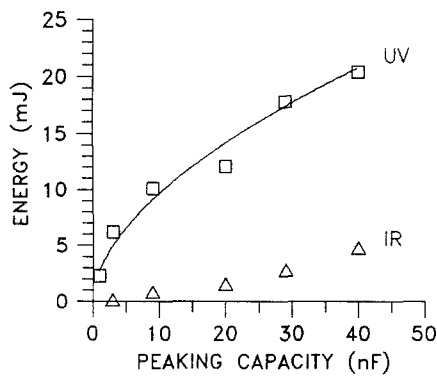


Fig. 8. UV and IR output energy vs peaking capacity.  $d=4$  cm,  $P=50$  Torr

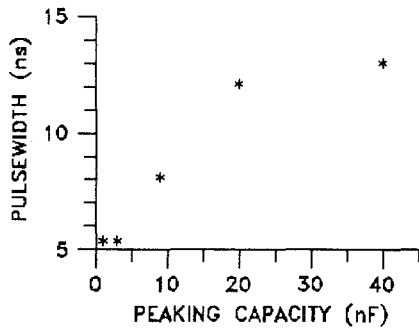


Fig. 9. UV pulsewidth vs peaking capacity.  $d=4$  cm,  $P=60$  Torr

is unaffected by the peaking capacitor as is experimentally observed.  $L$  is the total induction in the peaking circuit. The main contribution to  $L$  is probably due to the electrical connections between the capacitor plates and the electrodes [4]. Then we may suppose that  $L$  does not depend very much on  $C_p$ . Thus the laser output  $E$  is expected to be  $E \cong (C_p)^{1/2}$ . In Fig. 8 is shown the output energy fitting with that relation. On the other hand in the IR output the population inversion is the result of two pumping rates: cascade population from the second positive system and a direct electronic impact excitation. Thus it is not very surprising if the IR output does not fit that dependence.

The UV and the IR outputs have practically the same pulsewidth. The pulsewidth also grows with  $C_p$  (Fig. 9) attaining a peak power of 1.5 MW in the UV and 0.4 MW in the IR. The current pulse width is  $\Delta i \cong (LC_p)^{1/2}$  and this dependence is roughly that observed in the UV output pulsewidth.

The IR and UV pulse energy dependence on the N<sub>2</sub> pressure is shown in Fig. 10. The maximum IR pulse

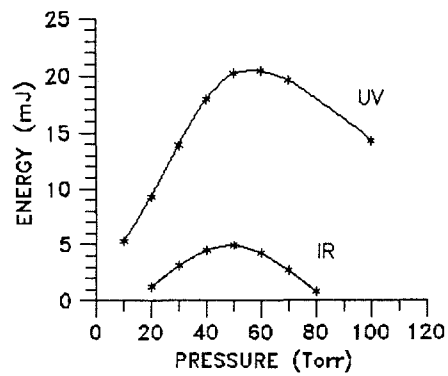


Fig. 10. UV and IR output energy vs N<sub>2</sub> pressure.  $d=4$  cm,  $C_p=40$  nF

energy is 5 mJ at a pressure of 50 Torr. In the UV pulse we attained 20.5 mJ when the pressure was 60 Torr.

### 3. Conclusions

We have designed and experimented with a charge transfer high energy transversal discharge N<sub>2</sub> laser. The laser is of a compact open design, easy to improve, and uses no unreliable elements such as water capacitors [2].

Using pure N<sub>2</sub>, we were able to obtain simultaneous operations in the first and second positive systems. A pulse energy of 20.5 mJ (1.5 MW) in the UV and 5 mJ (0.4 MW) in the IR were measured. In the infrared the output power is four times higher than the highest reported in self-sustained discharges [5]. This performance may easily be improved by increasing the capacity  $C_p$ , the electrode separation and possibly by changing the diameter of the upper electrode. A higher output energy may also be expected by the addition of attachers to the N<sub>2</sub> as in [2].

We are presently developing an improved version of this design in order to get higher pulse energies.

### References

1. E. Armandillo, A.J. Kearsley: *Appl. Phys. Lett.* **41**, 611 (1982)
2. U. Rebhan, J. Hildebrandt, G. Skopp: *Appl. Phys.* **23**, 341 (1980)
3. B. Oliveira dos Santos, J.B. de Oliveira e Souza, C.A. Massone: *Appl. Phys. B* **41**, 241 (1986)
4. A.J. Smith, K.H. Kwek, T.Y. Tou, A.V. Gholap, S. Lee: *IEEE J. QE-23*, 283 (1987)
5. R.S. Kunabenchi, M.R. Gorbali, M.I. Savadatti: *Nitrogen Lasers* (Pergamon, Oxford 1986) pp. 259-329
6. J.I. Levatter, S.C. Lin: *Appl. Phys. Lett.* **25**, 703 (1974)
7. T. Sakurai, T. Watanabe: *J. Appl. Phys.* **59**, 4007 (1986)